ELSEVIER

Journal of Molecular Catalysis A: Chemical 145 (1999) 237–244

JOURNAL OF MOLECULAR CATALYSIS A: CHEMICAL

www.elsevier.com/locate/molcata

Solid acid catalysts from clays Part 3: benzene alkylation with ethylene catalyzed by aluminum and aluminum gallium pillared bentonites [1]

Maurizio Lenarda *, Loretta Storaro, Giuliano Pellegrini, Luca Piovesan, Renzo Ganzerla

Dipartimento di Chimica, Università di Venezia Ca' Foscari, Dorsoduro 2137-30123 Venezia, Italy

Received 22 September 1998; accepted 10 December 1998

Abstract

A montmorillonite pillared with aluminum (APM) or aluminum/gallium polyoxycations (AGPM) and their respective repillared derivatives (AP2M and AGP2M) were prepared. The materials were characterized by chemical analysis, X-ray diffraction, N_2 adsorption–desorption. The surface acidity was evaluated by FT-IR spectroscopy of adsorbed pyridine and from the analysis of the product distribution of the 1-butene gas phase isomerization. The catalytic activity for the alkylation of benzene with ethylene to produce ethyl benzene was determined and correlated with the samples acidity. The derivatives pillared with $Al_{12}Ga$ mixed pillars resulted to be the more active catalysts.

Keywords: Alkylation; Ethylbenzene; Acidity; Pillared clays

1. Introduction

The Friedel–Crafts reaction is probably one of the more important reactions in organic chemistry. The reaction is catalyzed by both Brønsted and Lewis acid centres [2,3]. Traditional Friedel–Crafts processes employ mineral acids such as HF and H_2SO_4, or Lewis acids such as $AlCl_3$ and BF_3. The use of these substances involves technological and environmental problems due to their corrosive nature, the difficulty of recycling and the formation of large amounts of harmful wastes, with consequent economic and environmental problems. The present tendency is to replace these conventional catalysts by solid acids, which are less corrosive and harmful to the environment. Zeolites [4–6], acid treated clays [7,8] and pillared clays [9] can exhibit acidities close to those of traditional mineral acids solutions. The alkylation of benzene or toluene with light hydrocarbons over acidic catalysts for the production of alkylaromatics is a process of industrial significance [6,10,11].

Protonated or rare earth exchanged faujausites were used in the alkylation of benzene with ethylene ([10] and references therein). More recently, the liquid-phase alkylation of benzene with ethylene was studied on BEA-zeolite [6]. The alkylation of benzene with propilene is successfully catalyzed by silicoalluminophos-

* Corresponding author. Tel.: +39-41-2578562; Fax: +39-41-2578517; E-mail: lenarda@unive.it

[1] Part1: M. Perissinotto, M. Lenarda, L. Storaro, R. Ganzerla, J. Mol. Catal. A 121 (1997) 103; Part 2: Ref. [1].

1381-1169/99/$ - see front matter
PII: S1381-1169(99)00019-9

phates ([10] and references therein) or cation exchanged aluminum pillared clays [1].

In this work we studied the catalytic activity for the liquid-phase alkylation of benzene with ethylene to produce ethyl benzene of a montmorillonite pillared with aluminum or aluminum/gallium polyoxycations (APM and AGPM) and their respective repillared derivatives (AP2M and AGP2M).

2. Experimental

2.1. Characterization methods

2.1.1. Elemental analyses

Elemental analyses were accomplished by Atomic Adsorption Spectroscopy with a Perkin-Elmer PE 3100 instrument.

2.1.2. Thermogravimetric analyses

Thermogravimetric analyses were obtained with a Simultaneous Thermal Analyser STA 429 Netzsch using samples weighting about 50 mg. A heathing rate of 10 K/min with air (30 ml/min) as purging gas was used.

2.1.3. Nitrogen adsorption / desorption

Adsorption–desorption experiments using N_2 were carried out at 77 K on a Sorptomatic 1900 Carlo Erba porosimeter. Before each measurement the samples were outgassed at 423 K and 1.33×10^{-3} Pa for six hours. The N_2 isotherms were used to determine the specific surface areas (S.A.) using the BET equation. The α-plot method was used to calculate the micropore volume. The starting clay was used as reference material [12,13].

2.1.4. X-ray diffraction spectra

X-ray diffraction spectra were measured with a Philips diffractometer using the Cu-Kα radiation. The samples were disc shaped pressed powders and were previously treated at 673 K in a ventilated oven.

2.1.5. FT-IR measurements

IR spectral measurements were carried out in an evacuable Pyrex cell with CaF_2 windows. Pyridine adsorption experiments were performed as described by Occelli and Tindwa [14]. The clay was ground to a fine powder. Thirty milligrams of the sample were pressed at 4 tons, in order to get a self-supporting wafer. The wafers were mounted in the holder of the IR cell, and degassed by heating at 673 K and 1.33 Pa [15,16]. After cooling the wafers at room temperature, pyridine was adsorbed on the samples. The spectra were recorded after degassing the wafers under vacuum at 423 K and 1.33 Pa for two hours on a Nicolet Magna-IR 750 spectrometer.

2.1.6. Catalytic 1-butene isomerisation test

Catalytic 1-butene isomerisation tests were performed in a tubular glass flow microreactor. The catalyst samples were pretreated for 2 h in N_2 flow at 673 K. Experiments were performed at 673 K and $\tau = 2.4\ g_{(cat)} \cdot g^{-1}_{(1\text{-butene})} \cdot h$. The 1-butene was at 5% abundance in nitrogen and the time on stream was 120 min. The unconverted 1-butene and the reaction products were analyzed on line in a gas chromatograph (HP 5890 series II) equipped with a wide-bore $KCl/AlCl_3$ column ($\phi = 0.53$ mm, $l = 50$ m) and a flame ionization detector (FID).

The amount of coke was deduced from the weight loss of the spent catalyst during burning in air in the range 363–1073 K, measured by thermogravimetry (TG).

2.1.7. Catalytic alkylation of benzene with ethylene

The alkylation of benzene with ethylene was carried out at 453 K in a 250 ml magnetically stirred autoclave (reaction time 22 h) using 100 mg of catalyst, previously treated in air flow at 673 K for 20 h. A total of 1.40 g of ethylene, 20 ml of benzene (benzene/ethylene = 4.5) and 100 mg of catalyst were heated to 453 K and the system was pressurized with argon up to a total pressure of 45 bar [$\tau = 0.116$ (g_{catal}/

$g_{benzene+ethylene}) \times h$]. After 22 h of reaction the autoclave was cooled and the products were analyzed in a gas chromatograph (Chrompack CP) equipped with a wide-bore OV1 column ($\phi = 0.53$ mm, $l = 10$ m) and a flame ionization detector (FID), and a gas chromatograph (HP 5890 series II) equipped with a wide-bore $KCl/AlCl_3$ column ($\phi = 0.53$ mm, $l = 50$ m) and a flame ionization detector (FID).

2.2. Materials

Detercal P1™, the clay used in this study, was a natural calcium rich bentonite (montmorillonite 97%) of North African origin (Nador, Morocco), factory dried, ground and sieved, which was obtained from Industria Chimica Carlo Laviosa (Leghorn, Italy) (CEC = 84 meq/100 g).

Its structural formula, previously determined [17], is $[Ca_{0.13}\ Na_{0.43}\ K_{0.15}\ (Si_{7.56}\ Al_{0.44})(Al_{3.23}\ Fe_{0.22}\ Mg_{0.54})\ O_{20}\ (OH)_4]$. Chlorhydrol™, a commercial 5/6 basic aluminum chloride salt produced by Reheis was obtained as a kind gift from Eigenmann and Veronelli (Milan). Benzene was C. Erba reagent $\geq 99.5\%$ pure. Ethylene was supplied by SIAD. Gallium and Aluminum chlorides were Aldrich reagents.

2.2.1. Preparation of the Al_{13}- and $Al_{12}Ga$-pillared clay

Aluminum and aluminum/gallium pillared clays (APM and AGPM) ($d_{001} = 1.87$ and 1.85 nm) were synthesized by a slight modification of a published method [18]. The pillaring $Al_{12}Ga$ agent was prepared as described in the literature [19] from a 0.2 M aqueous solution of $AlCl_3 + GaCl_3$ ($Al/Ga = 12/1$) by gradual addition of an appropriate volume of a NaOH 0.5 M solution to obtain $OH/(Al + Ga) = 2.0$ ratio. The reaction mixture was then diluted with distilled water to yield $(Al + Ga) = 0.1$ M. The pH of the final solution was 3.7.

2.2.2. Preparation of the Al_{13}- and $Al_{12}Ga$-repillared clays

The cation exchange capacity (CEC) of the APM and AGPM samples was restored by treatment with NH_3 vapours and the above described pillaring process with aluminum and aluminum/gallium polyoxycations was repeated to give respectively AP2M and AGP2M.

3. Results and discussion

3.1. Pillared clays characterization

XRD profiles of the samples are presented in Fig. 1. The d_{001} basal spacing values, the surface areas and micropore volumes of all the pillared smectites are reported in Table 1.

All pillared clays presented, after calcination at 673 K, an intense and sharp d_{001} peak at ~ 1.85 nm with peak widths of about 0.25 nm indicating a high layer stacking order along the *c*-axis.

All the samples showed the well known micro-mesoporous binary pore distribution of the aluminum pillared smectites. Both $Al_{12}Ga$-pil-

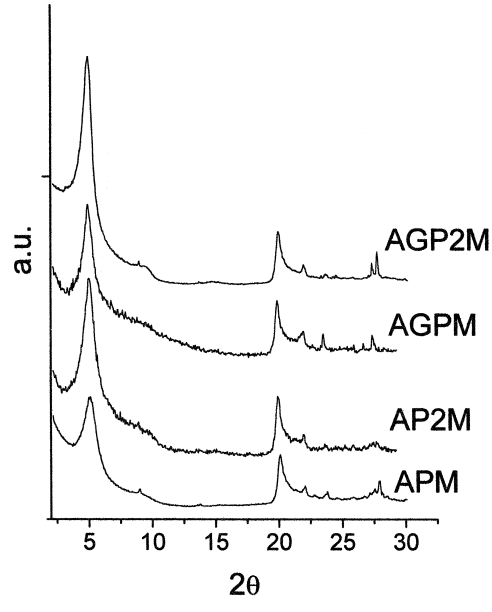

Fig. 1. X-Ray diffractograms of the pillared and repillared clays.

Table 1
Basal spacings (d_{001}), specific surface areas (S.A.), micropore volumes (V_μ) of the PILCs

Sample	d_{001} nm	S.A. m^2/g	V_μ cm^3/g
APM	1.87	370.0	0.16
AP2M	1.87	252.1	0.10
AGPM	1.85	382.8	0.16
AGP2M	1.84	322.5	0.14

lared clays showed BET surface areas and micropore volumes higher than the Al_{13}-pillared derivatives. Various techniques have been used to understand the nature and location of the Ga sites of gallium doped aluminum pillared clays [19–22]. It was demonstrated by MAS-NMR, that the central tetrahedral Al^{3+} of the pillaring Keggin type ion is replaced by a tetrahedral Ga^{3+} ion [21,22].

The intercalation of $GaAl_{12}$ species into a montmorillonite appears to give origin to a pillared clay more microporous and structurally more stable to high temperatures as is proved by the XRD spectra shown in Fig. 2.

It was found that Ga-doped pillared clays have a lower number of pillars per gram of clay compared to the Al_{13} pillared derivatives and that [21,22] the slightly larger ionic radius of Ga^{3+} ion makes the $GaAl_{12}$ structure more symmetric than that of the parent aluminum oligomer.

When the APM and AGPM pillared clays were reintercalated, the exchangeable cations regenerated by treatment with NH_3 vapours were replaced by Al_{13}- and Al_{12}Ga-polyoxycations.

The repillared clays showed a XRD pattern very similar to that of the mono pillared derivatives (Fig. 1) but with lower surface area, most probably because of the loss of microporosity caused by the increased number of the pillars.

The surface area of the APM decreased from 370.0 to 252.1 m^2/g after repillaring, whereas the surface area of the AGPM decreased only from 382.8 to 322.5 m^2/g.

It was reported [21,23] that repillaring with Al_{12}Ga-polyoxycations causes a 30% increase of the pillar number, while only 20% more pillars were found in clays repillared with Al_{13}-polyoxycations.

The decrement of the micropore volume after repillaring was 28.6% for the Al pillared samples and 12.5% for the AlGa derivatives.

As illustrated in Scheme 1, during the pillaring process the polycations (little white rectangles) prop open a large amount of the clay layers, creating an interlayer space (Scheme 1 A). Nevertheless, some layers still remain only partially open or completely closed (Scheme 1 B and C). During the reintercalation process further diffusion of polyoxycations in the interlayer space can integrate the pillaring process leading to higher pillar density (Scheme 1 A′) and/or to completion of the process that did not occur or occurred only in part (little grey rectangles). Consequently, the micropore volume loss after repillaring is more pronounced for the higher pillar density Al pillared clays in comparison with the lower pillar density AlGa clays.

3.2. Surface acidity evaluation

The surface acidity was evaluated by FT-IR spectroscopy of adsorbed pyridine [14–16] and

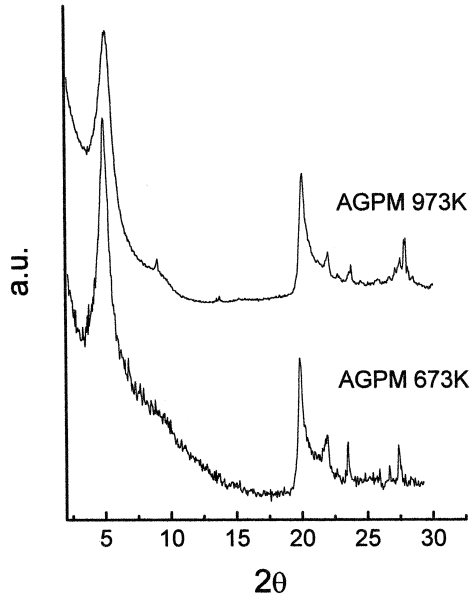

Fig. 2. X-Ray diffractograms of the Al_{12}Ga-pillared sample calcined at 673 or 973 K.

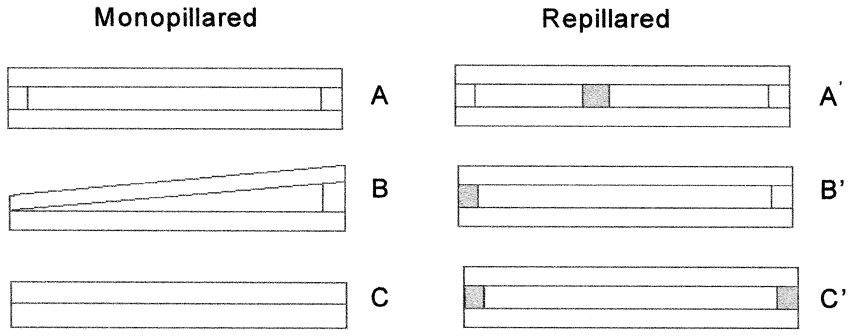

Scheme 1.

from the analysis of the product distribution of the 1-butene gas phase isomerization [17,24–26].

3.2.1. FT-IR study of adsorbed pyridine

The IR spectra of pyridine adsorbed on APM and AGPM pellets after evacuation at 423 K are shown in Fig. 3.

A general decrease of the IR bands intensity in the 1700–1400 cm^{-1} region was observed going from APM to AGPM, in particular of the 1545 cm^{-1} and 1450 cm^{-1} bands typical of the pyridine bonded to, respectively, the Brønsted and Lewis acid sites.

3.2.2. Catalytic 1-butene isomerisation test

The distribution of some of the reaction products (isobutene, *n*- and isobutanes, and the products of coking) can give information on the strength and type of the acid sites.

The results are summarised in Table 2.

The skeletal isomerisation of *n*-butenes implies the transposition of a *sec*-butyl carbenium ion to a *tert*-butyl carbenium ion. This process necessitates rather strong Brønsted acid sites [27,28]. Lewis and very strong Brønsted acid centers are known to promote coke formation [29]. The hydrogenated compounds, *n*-butane and isobutane, are found among the other products. Their presence can be explained by a cracking reaction of butene oligomeric carbenium ions or, more probably, in our conditions, by a direct hydrogenation of the butene isomers through hydride transfer to the corresponding monomeric carbenium ions. In order to evaluate the skeletal isomerisation activity of the samples, the amount of isobutene produced should be added to that of isobutane, assuming that the last originates from isobutene.

The total skeletal isomerisation activity and the coke were divided for the BET area values in order to normalize the data of catalysts with very different surface areas.

The overall activity of APM clay decreased after repillaring whereas that of AGPM was only slightly modified.

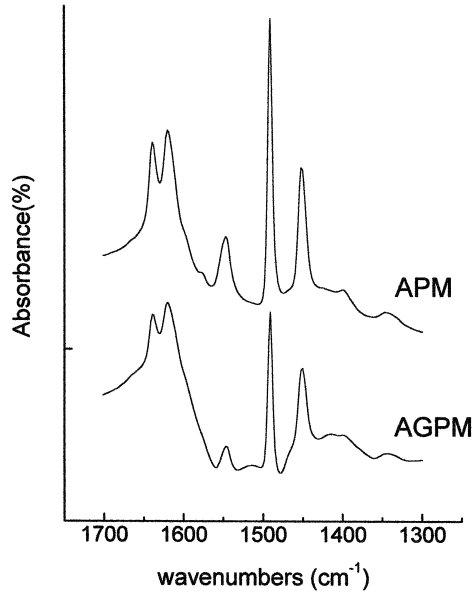

Fig. 3. IR spectra of pyridine adsorbed on the Al_{13}- and $Al_{12}Ga$-pillared clays.

Table 2
Catalytic conversion of the 1-butene on the pillared and repillared samples

Sample	Product gas composition (%)				Conv.	(§) S_L	(§§§) coke	(§§) *a*	(§§§§) *b*
	Iso butane	Normal butane	Iso butene	Normal butene					
APM	1.0	0.5	16.0	82.5	17.5	91.1	3.8	4.6	1.0
AP2M	0.6	0.4	8.5	90.5	9.5	89.5	8.4	3.6	3.3
AGPM	1.1	0.7	12.1	86.1	13.9	87.0	1.8	3.4	0.5
AGP2M	0.7	0.5	11.1	87.7	12.3	90.2	3.3	3.6	1.0

(§) = (wt.% isobutene)$_{effluent}$/[(wt.% *n*-butenes)$_{feed}$-(wt.% *n*-butenes)$_{effluent}$)].
(§§) a = iso total/S_{BET} * 100.
(§§§) coke = g coke/g cat * 100.
(§§§§) b = coke/S_{BET} * 100.

As shown in Table 2 the APM pillared clay was more active in the skeletal isomerization (isobutene and isobutane formation), that is catalyzed by strong Brønsted acid sites, while AP2M was the less active. Nevertheless, AP2M produces the highest amount of carbonaceous compounds (8.4 wt.%). This indicates that the repillaring process leads to a clay with a larger number of Lewis acid sites which forms large coke amounts most probably responsible for the catalyst deactivation.

The AGPM and AGP2M clays show a behaviour laying between these two Al_{13}-pillared derivatives.

3.3. Catalytic alkylation of benzene with ethylene

The alkylation of benzene with ethylene was carried out at 453 K for 22 h in a stirred batch reactor. The high ratio benzene/ethylene = 4.5 and the relatively low temperature were chosen to favor the mono-alkylated product and to avoid the formation of poly-alkylated derivatives [4]. A selectivity above 80% in ethylbenzene was obtained for all samples. Ethylene polymerization products were never detected.

A normalized reaction time τ is defined as $\tau = WF^{-1}t$, where W is the catalyst weight (g), F is the amount of benzene-olefin mixture (g), and t is the reaction time (h). A t of 0.116 h was utilized.

The results are reported in Table 3.

In Fig. 4 the time dependence of the ethylene conversion on AGPM and AGP2M clays is showed.

Both AGPM and AGP2M clays resulted very active, the latter being the best catalyst.

Reactivity and spectroscopic data confirmed that the chemical properties of Al and Al/Ga pillared montmorillonites were modified by repillaring, while the clay structure appeared only slightly affected. The slight decrease of the specific surface area values (Table 1) is attributable to the filling of the interlamellar space by the added pillars. The samples with only Al_{13} pillars show more intense IR bands at 1540 and 1450 cm^{-1}, corresponding to Brønsted and Lewis acid centers, indicating that they have a larger number of pillars per gram of material in comparison with the Al/Ga derivatives (Fig. 3). For increasing pyridine desorption temperatures the band at 1450 cm^{-1} assigned to Lewis cen-

Table 3
Ethylene conversion, selectivity and yield in ethylbenzene, in the alkylation of benzene with ethylene catalyzed by the Al_{13}- and $Al_{12}Ga$-pillared and repillared clays

Sample	Ce%	Seb%	Yeb%
APM	8	86	7
AP2M	13	82	11
AGPM	25	86	22
AGP2M	30	84	25

Ce% = Percent ethylene conversion.
Seb% = Ethylbenzene/alkylation products molar ratio × 100.
Yeb% = Percent ethylbenzene yield.

ters weakens faster in the APM sample in comparison with AGPM, indicating that the Lewis centers on the $Al_{12}Ga$-pillared sample are stronger.

The 1-butene isomerisation test gives additional information on the relative number and strength of the acid sites. The Al_{13}-pillared clays have more pillars compared with the $Al_{12}Ga$-pillared derivatives and this justifies the higher number of Lewis acid sites responsible for the coke formation (Table 2). On the other hand, the lower number of pillars in the $Al_{12}Ga$-pillared clays implies less, but stronger Lewis acid sites. This can be due to the charge polarization caused by the more electronegative gallium on Al^{VI} (Al^{VI}–O–Ga^{IV}–) compared with Al^{VI} (Al^{VI}–O–Al^{IV}–) [21,23].

An attempt to correlate the activity in the benzene alkylation with the acid properties of various PILCs was made but there is no apparent dependence of the catalytic activity on the relative amount of strong Brønsted or Lewis

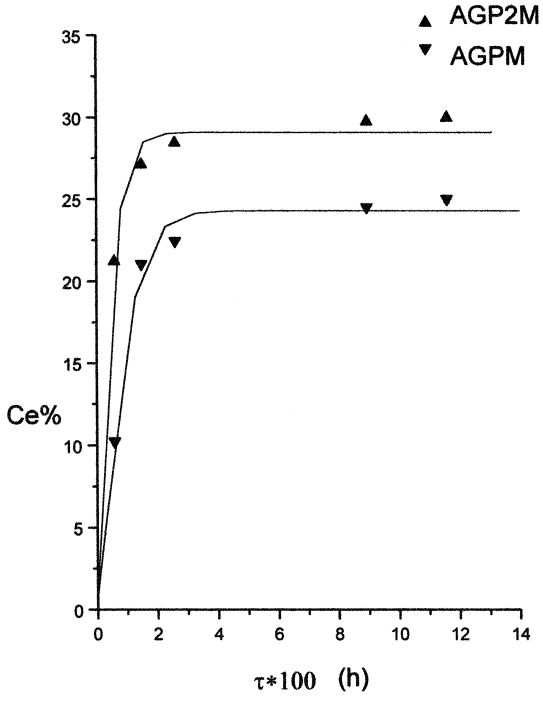

Fig. 4. Influence of the repillaring process on the ethylene conversion.

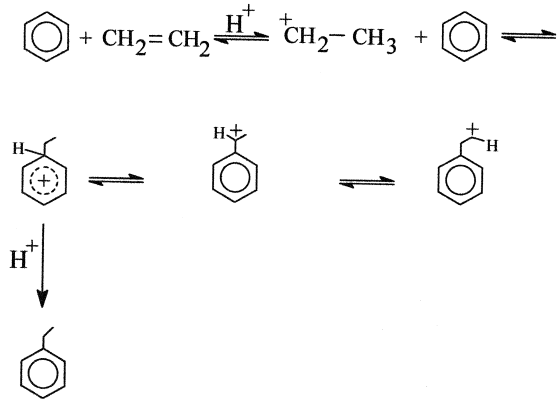

Scheme 2.

acid centers. Nevertheless, it is well known that the Friedel–Crafts alkylation of benzene with ethylene over acidic zeolites takes place via the generally accepted carbenium ion mechanism illustrated in Scheme 2.

On the basis of this mechanism, the ethylene molecule is protonated by the Brønsted acid sites to a carbenium ion that generates, by electrophilic attack on the aromatic π-electrons, a mono or polyalkylbenzenium ion. The desorption of the latter and the loss of the proton gives the alkylated aromatic and restores the Brønsted acid sites.

It was assumed that the reaction proceeds according to the Langmuir–Hinshelwood (LH) mechanism [30], the rate determining step being the reaction between the benzene molecule adsorbed on the aprotic sites and the ethylene molecule adsorbed on the protonic sites. The $Al_{12}Ga$-mono pillared and repillared clays, that have stronger aprotic sites probably better coordinate the benzene molecules allowing an easier reaction with the ethylene adsorbed on the protonic sites.

4. Conclusions

Montmorillonites pillared with aluminum (APM) or aluminum/gallium polyoxycations (AGPM) and their respective repillared derivatives (AP2M and AGP2M) are all active cata-

lysts of the alkylation of benzene with ethylene to produce ethylbenzene.

The title reaction was found to occur with good yield and selectivity, in particular on AGPM and AGP2M samples, the latter being the more active catalyst. The higher activity of the $GaAl_{12}$-pillared samples must be related to the presence of stronger Lewis acid sites on the pillars.

Acknowledgements

The financial support of M.U.R.S.T. is acknowledged.

References

[1] A. Geatti, M. Lenarda, L. Storaro, R. Ganzerla, M. Perissinotto, J. Mol. Catal. A 121 (1997) 119.
[2] Kirk-Othmer, Encyclopedia of Chemical Technology, Wiley, New York, 1978.
[3] G.A. Olah, Friedel-Crafts Chemistry, Wiley, 1973.
[4] W.W. Kaeding, R.E. Holland, J. Catal. 109 (1988) 212.
[5] C. Gauthier, B. Chiche, A. Finiels, P. Geneste, J. Mol. Catal. 50 (1989) 219.
[6] G. Bellussi, G. Pazzucconi, C. Perego, G. Girotti, G. Terzoni, J. Catal. 157 (1995) 227.
[7] C.N. Rhodes, D.R. Brown, J. Chem. Soc. Faraday Trans. 88 (15) (1992) 2269.
[8] C. Cativiela, J.I. García, M. García-Matres, J.A. Mayoral, F. Figueras, J.M. Fraile, T. Cseri, B. Chiche, Appl. Catal. A 123 (1995) 273.
[9] J.R. Butruille, T.J. Pinnavaia, Catal. Today 14 (1992) 141.
[10] P.S. Smirniotis, E. Ruckenstein, Ind. Eng. Chem. Res. 34 (1995) 1517.
[11] K. Weissermel, H.J. Arpe, Industrial Organic Chemistry, 3rd edn., VCH, 1997.
[12] S.J. Gregg, K.S.K. Sing, Adsorption, Surface Area and Porosity, 2nd edn., Academic Press, London, 1982.
[13] M.S. Baksh, E.S. Kikkinides, R.T. Yang, Ind. Eng. Chem. Res. 31 (1992) 2181.
[14] M.L. Occelli, R.M. Tindwa, Clays and Clay Min. 31 (1983) 22.
[15] J. Datka, J. Chem. Soc. Faraday Trans. 1 (76) (1980) 2437.
[16] J. Datka, J. Chem. Soc. Faraday Trans. 1 (77) (1981) 1309.
[17] L. Storaro, M. Lenarda, M. Perissinotto, V. Lucchini, R. Ganzerla, Micropor. Mesop. Mater. 20 (1998) 317.
[18] L. Storaro, M. Lenarda, R. Ganzerla, A. Rinaldi, Micropor. Mater. 6 (1996) 55.
[19] F. Gonzales, C. Pesquera, C. Blanco, I. Benito, S. Mendioroz, Inorg. Chem. 31 (1992) 727.
[20] S.M. Bradley, R.A. Kydd, J. Catal. 141 (1993) 239.
[21] M.J. Hernando, C. Pesquera, C. Blanco, I. Benito, F. Gonzales, Chem. Mater. 8 (1996) 76.
[22] W. O'Neil Parker Jr., R. Millini, I. Kiricsi, Inorg. Chem. 36 (1997) 571.
[23] X. Tang, W.-Q. Xu, Y.-F. Shen, S.L. Suib, Chem. Mater. 7 (1995) 102.
[24] J. Goldwasser, J. Engelhardt, W.K. Hall, J. Catal. 71 (1981) 381.
[25] M. Guisnet (Ed.), Catalysis by Acids and Bases, Elsevier Science Publishers, 1985, pp. 283.
[26] P. Patrono, A. La Ginestra, G. Ramis, G. Busca, Appl. Catal. A 107 (1994) 249.
[27] J. Datka, J. Chem. Faraday Trans. 1 (77) (1981) 2633.
[28] M. Trombetta, G. Busca, S. Rossini, V. Piccoli, U. Cornaro, J. Catal. 168 (1997) 334.
[29] K. Moljord, P. Magnoux, Guisnet, Appl. Catal. A 122 (1995) 21.
[30] P.G. Smirniotis, E. Ruckenstein, Ind. Eng. Chem. Res. 34 (1995) 1517.